Environ Monit Assess (2022) 194:269
https://doi.org/10.1007/s10661-022-09870-4

Ecological degradation and non-carcinogenic health risks of potential toxic elements: a GIS-based spatial analysis for Doğancı Dam (Turkey)

Şakir Fural · Serkan Kükrer · İsa Cürebal · Dilek Aykır

Received: 3 November 2021 / Accepted: 17 February 2022

Abstract This study was carried out to determine the ecological degradation and non-carcinogenic health risks at Doğancı Dam, Bursa, Turkey. Potentially toxic element (PTE) concentrations (ppm) were as follows: Fe (55.030) > Al (27.220) > Mn (1053) > Cr (181) > Ni (180) > Zn (95) > Cu (62) > As (17) > Pb (11) > Cd (0.20) > Hg (0.108). As, Pb, Cd, and Hg were enriched anthropogenically, while other PTEs were of natural origin. The contamination severity index (CSI) indicated a moderate PTE contamination in the dam, mostly due to lithogenic effects. According to the modified hazard quotient (mHQ), ecological risk was identified at the level of extreme severity for Ni of lithological origin, of high severity for Cr of considerable severity for As of anthropogenic origin, and of moderate severity for Cu. According to the ecological contamination index (ECI), the dam had an ecological risk of a slight-to-moderate contamination. Health risk index showed no non-carcinogenic health risks in the dam. Mining, highways, and agricultural activities were identified as the primary anthropogenic drivers to be monitored. The ongoing anthropogenic activities in the Nilüfer Stream basin and natural factors affect the ecological degradation and non-carcinogenic health risk level of the dam.

Keywords Environmental monitoring · Ecological risk · Potential toxic element pollution · Human health risk assessment · Geographical information system

Introduction

Metals are divided into two different groups; as essential (e.g., Al, Fe, Mn, and Zn) and non-essential elements (e.g., Hg, Cd, Pb, and As). While essential elements are very important for the Earth's crust and living structures, non-essential elements are used in anthropogenic activities. However, both element groups may demonstrate toxic properties as a result of anthropogenic effects. Metals with the risk of harming the ecosystem and human health due to enrichment by anthropogenic effects are called potential toxic elements (PTEs) (Ustaoğlu & Islam, 2020; Wei & Cen, 2020). Due to anthropogenic processes such as industry, mining, transportation networks, agriculture, and settlements (Lorenzana et al., 2008), ecological and health risk problems are caused by PTEs in aquatic ecosystems such as streams (Ustaoğlu et al., 2020; Xiao et al., 2021), lakes (Wang et al., 2016; El-Alfy et al.,

Ş. Fural (✉)
Department of Geography, Faculty of Arts and Sciences, Kırşehir Ahi Evran University, Kirsehir, Turkey
e-mail: furalsakir@gmail.com

S. Kükrer · D. Aykır
Department of Geography, Faculty of Humanities and Literature, Ardahan University, Ardahan, Turkey

İ. Cürebal
Department of Geography, Faculty of Arts and Sciences, Balıkesir University, Balikesir, Turkey

Published online: 10 March 2022

2020; Niu et al., 2020), lagoons (Hu et al., 2018; Kükrer et al., 2020), bays (Elsagh et al., 2021; Haghshenas et al., 2020; Soliman et al., 2018), and dams (Farsani et al., 2019; Fural et al., 2021). PTE pollution in natural wetlands disrupts the ecological balance by harming wild fauna species (Marzio et al., 2019). PTE pollution in wetland sediments can cause health problems by passing into the human body by the consumption of water and living things that feed on sediment such as fish (Magni et al., 2021; Nargis et al., 2019). PTE can be released back into water from sediment depending on biological and geochemical conditions (Wang et al., 2012; Yuan et al., 2014). The release of PTEs enriched by anthropogenic effects into the water can create serious problems for the dam's ecosystem and for the people who take advantage of dams in various ways, such as via water consumption, fishing, and agricultural irrigation. Dam water reaches people directly through the water network (Fural et al., 2020). Ecological risks caused by PTE in dams whose water level has decreased due to climatic conditions in recent years (Aydın et al., 2017) may make it difficult for people to access clean and safe water in the coming years.

While approximately one-fifth of the world's population (1.2 billion people) had difficulty in accessing clean water in 2007, this rate is estimated to increase to two-thirds in 2025 (FAO, 2007). Globally, the amount of water consumption was one billion m^3 in 1940 and four billion m^3 in 1990, and is estimated to exceed eight billion m^3 after 2030 (WWF, 2014). In spite of the rapidly increasing need for water, the accelerated depletion of water resources due to climate change and anthropogenic processes such as PTE pollution indicates that the world is rapidly drifting towards a crisis in accessing clean water.

Countries in the Mediterranean basin are not rich in water due to their geological, geomorphological, hydrographic, climatic, and demographic characteristics. Unless Turkey protects its water resources well, it may suffer from water scarcity in the short term (Falkenmark et al., 1989). Hence, ecological risk studies should be carried out on a local, regional, and global scale. In particular, wetlands should be continuously monitored against all anthropogenic effects, especially for ecological degradation and health risks originating from PTEs.

In this study, Doğancı Dam, which provides drinking water to Bursa, the fourth largest metropolis in Turkey, was chosen as the study area. Mining, agriculture, highways, and settlement are the prominent anthropogenic activities in the Doğancı Dam basin. Land-use and cover data show that 25% of the watershed has intense anthropogenic activity (Fig. 1). The potential of mining and the highway near the dam to create ecological degradation, and health risk problems are quite high (Chakraborty et al., 2021; Lu et al., 2019). For this reason, it is necessary to determine the ecological effects of all land use types on the dam, especially mining and the highway, and offer solutions to the identified problems. In this study, the aforementioned problems are discussed and suggestions for solutions are presented.

This study set out to achieve three main objectives. Firstly, the ecological, toxicological, and non-carcinogenic health risk level created by PTEs (Al, As, Cd, Cr, Cu, Fe, Hg, Ni, Pb, Mn, and Zn) were analyzed in Doğancı Dam surface sediments using various indices, statistical methods, and geographical information systems (GIS). Secondly, scientific monitoring studies to avert the risk of PTE concentration reaching a non-carcinogenic health risk level that may pose a public health threat were initiated. Finally, contributions to and insights into the sustainable use of Doğancı Dam, an extremely important resource on a local, regional, and global scale, were posed so as to protect the population from anthropogenic effects.

Material and method

Study area

Doğancı Dam was built in the western part of Turkey south of Bursa city on the Nilüfer Stream in 1983 to provide drinking water (Fig. 1). The volume of the dam is 2.520.000 m^3, its crest (body) height is 65 m, and its volume at maximum water level is 37.80 hm^3 with an area of 1.55 km^2 at a normal water level. The dam, which is fed by Nilüfer Stream, Kapıkaya Creek, and seasonal stream tributaries, provides 125 hm^3 of drinking water to Bursa annually (BUSKI, 2021). Metamorphic, volcanic, and sedimentary rock formations exist in the basin, which covers an area of 450 km^2 (MTA, 2021).

A total of 74.62% of the basin consists of natural areas: 56.65% (255.70 km^2) of the basin is forest, 11.35% (110.41 km^2) is thicket, 2.97% (13.40 km^2) is rocky terrain, 2.78% (12.55 km^2) is natural pastureland,

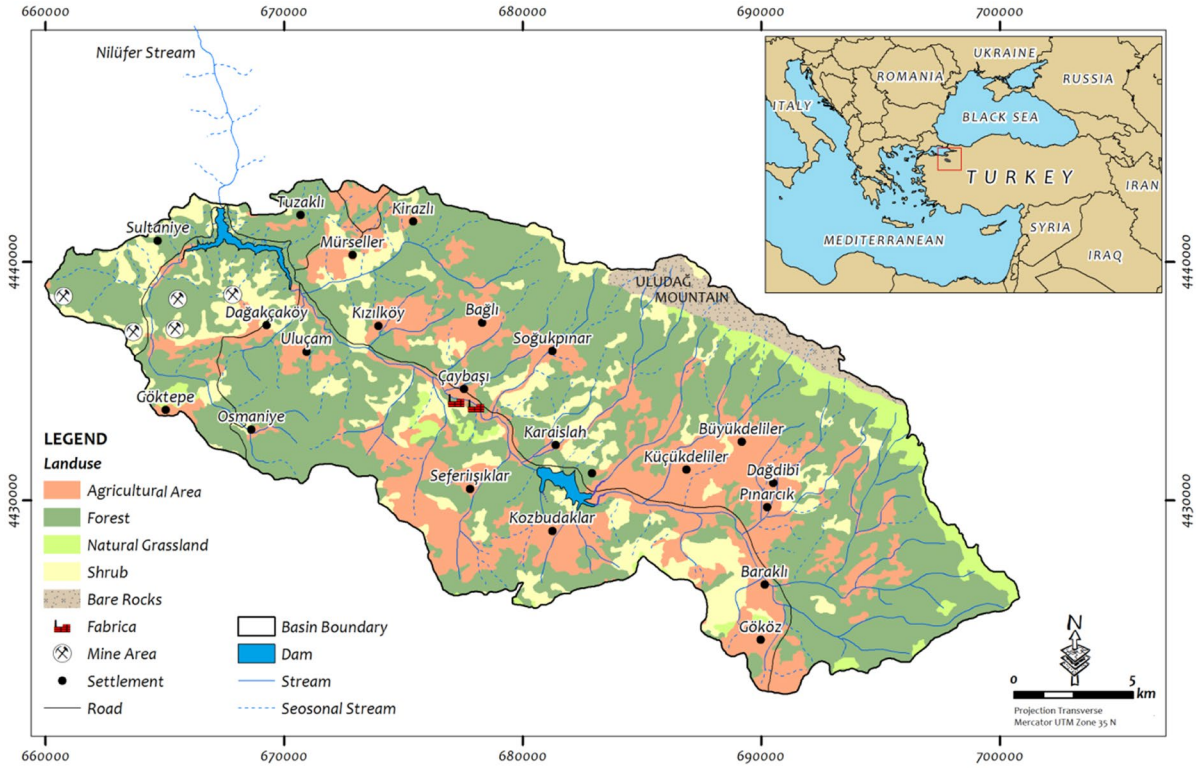

Fig. 1 Location of dam, land-use, and cover map

and 0.87% (3.70 km^2) is water surface. A total of 24.50% (110.41 km^2) of the basin is used as agricultural land, 0.55% (1.49 km^2) as mines, 0.28% (1.26 km^2) as settlements, and 0.10% (0.40 km^2) is used in the form of roads (CORINE, 2018). Anthropogenic activities are carried out in 25.38% of the basin (Fig. 1).

Sediment sampling and laboratory work

Sediment sampling was carried out in the summer of 2019 (24.08.2019). Sediment samples were used in the study because the PTE concentration in the sediment can remain constant for a long time (Ftrstner, 1976; Luczynskaa & Kang, 2018). Surface sediment samples were taken from 11 points, while rock samples were taken from 6 points in different geological formations in the basin to determine PTE background values. Wet sediment samples were dried in an oven at 60 °C for 24 h for total organic carbon (TOC) and PTE analyses. Dry sediments were pulverized in a mortar. PTE analysis was carried out by ICP-MS Bureau Veritas Analytical Labs in Canada. Reference material, duplicate measurements, and blind sampling measurements were performed to test the validity of the analyses. The recovery values of PTE measurements varied between 95.08 and 108.84%. TOC analysis was done using the Walkley Black Titration method (Gaudette et al., 1974), while CDP measurements were performed using the acetone extraction application and spectrophotometric method (Lorenzen, 1971). $CaCO_3$ analysis was done with a Scheibler Calcimeter (Schlichting & Blume, 1966).

Analytical procedure

Enrichment factor (EF), contamination factor (CF), modified degree of contamination (mCd), and geo-accumulation index (I_{geo}) are used to identify natural and anthropogenic sources of PTE.

EF is calculated according to formula 1:

$$\mathrm{EF} = \frac{(C_i/C_{ref})_{sample}}{(B_i/B_{ref})_{background}} \quad (1)$$

where C_i refers to the PTE concentration, C_{ref} is the reference PTE concentration, B_i is the regional background value of PTE, and B_{ref} is the background value of the reference PTE. EF findings are classified as follows: EF < 2 no enrichment/minor enrichment, EF = 2–5 a moderate enrichment, EF = 5–20 a severe enrichment, EF = 20–40 a very severe enrichment, and EF > 40 an extremely severe enrichment (Sutherland, 2000).

CF is calculated according to formula 2:

$$\mathrm{CF} = \mathrm{C}_i/\mathrm{C}_{\mathrm{background}} \tag{2}$$

where C_i is the PTE concentration and $C_{background}$ is the background value of PTE. CF data are classified as follows: CF < 1 low contamination, 1 ≤ CF < 3 moderately contaminated, 3 ≤ CF < 6 considerable contamination, and CF > 6 a very high contamination (Hakanson, 1980).

mCd is the modified form of CF and calculated according to formula 3 (Abrahim & Parker, 2008):

$$\mathrm{mCd} = \frac{\sum_{i=1}^{n} \mathrm{CF}}{\mathrm{n}} \tag{3}$$

where n is the number of PTEs used in the analysis. mCd is classified as follows: 1.5 ≤ mCd < 2 low degree of contamination, 2 ≤ mCd < 4 moderate degree of contamination, 4 ≤ mCd < 8 high degree of contamination, 8 ≤ mCd < 16 very high degree of contamination, 16 ≤ mCd < 32 extremely high degree of contamination, and mCd ≥ 32 ultra high degree of contamination. (Abrahim & Parker, 2008).

I_{geo} is calculated according to formula 4:

$$\mathrm{I}_{\mathrm{geo}} = \log_2 \frac{Ci}{(Bm * 1.5)} \tag{4}$$

where Ci is the PTE concentration and Bm is the continental crust value of PTE. I_{geo} is classified as follows: $I_{geo} \le 0$ uncontaminated, $0 < I_{geo} < 1$ uncontaminated to moderately contaminated, $1 < I_{geo} < 2$ moderately contaminated, $2 < I_{geo} < 3$ moderately to strongly contaminated, $3 < I_{geo} < 4$ strongly contaminated, $4 < I_{geo} < 5$ strong to extremely contaminated, and $I_{geo} \ge 5$ extremely contaminated (Müller, 1969).

Toxic risk index (TRI_i) was used to detect toxic risks of each PTE, as follows (Zhang et al., 2016). TRI_i is calculated according to formula 5:

$$TRI_i = \sqrt{\frac{((C_i/TEL)^2 + (C_i/PEL)^2)}{2}} \tag{5}$$

where C_i represents the PTE concentration, TEL represents "threshold effect level," and PEL represents "probable effect level"(MacDonald et al., 1997). Since there is no TRI_i risk index scale, integrated TRI was used in risk assessment in this study.

TRI is calculated according to formula 6:

$$TRI = \sum_{i=1}^{n} TRI_i \tag{6}$$

where TRI_i is the toxic risk index of a PTE, i is the PTE concentration, and n is the number of PTEs used in the analysis. TRI is the total toxic risk value. TRI data are classified thus: TRI ≤ 5 no toxic risk, 5 < TRI ≤ 10 a low toxic risk; 10 < TRI ≤ 15 a moderate toxic risk; 15 < TRI ≤ 20 a considerable toxic risk; and TRI > 20 a very high toxic risk (Zhang et al., 2016).

mHQ is calculated with the method of comparing the ecological and toxicological effects of PTE stored in the sediment with different threshold levels (Benson et al., 2018; MacDonald et al., 2000). mHQ is calculated according to formula 7:

$$\mathrm{mHQ} = \left[\mathrm{C_i}\left(\frac{1}{\mathrm{TEL}} + \frac{1}{\mathrm{PEL}} + \frac{1}{\mathrm{SEL}}\right)\right]^{1/2} \tag{7}$$

where SEL is the severe effect level. mHQ findings are classified in the following manner: mHQ < 0.5 nil to very low severity of contamination, 0.5 ≤ mHQ < 1.0 very low severity of contamination, 1.0 ≤ mHQ < 1.5 low severity of contamination, 1.5 ≤ mHQ < 2.0 moderate severity of contamination, 2.0 ≤ mHQ < 2.5 considerable severity of contamination, 2.5 ≤ mHQ < 3.0 high severity of contamination, 3.0 ≤ mHQ < 3.5 very high severity of contamination, and mHQ > 3.5 extreme severity of contamination (Benson et al., 2018).

ECI is used to determine the integrated total ecological risk level. ECI provides an empirical approach to ecological risk assessment using principal component analysis/factor analysis and is calculated according to formula 8:

$$\mathrm{ECI} = B_n \sum_{i=1}^{n} mHQ_i \tag{8}$$

where B_n is the inverse of the eigenvalue obtained from the analysis of principal components. The ECI findings are classified in the following manner: ECI < 2 uncontaminated, 2 ≤ ECI < 3 uncontaminated to slightly contaminated, 3 ≤ ECI < 4 slightly to moderately contaminated, 4 ≤ ECI < 5 moderately contaminated, 5 ≤ ECI < 6 considerably to highly contaminated, 6 ≤ ECI < 7 highly contaminated, and ECI > 7 extremely contaminated (Benson et al., 2018).

CSI was developed to analyze the level of PTE contamination (Pejman et al., 2015), based on ERL (effects range low) and ERM (effects range median) (Long et al., 1998). CSI is calculated according to formula 9:

$$\mathrm{CSI} = \sum_{i=1}^{n} W_i \left[\left(\frac{C_i}{ERL_i} \right)^{1/2} + \left(\frac{C_i}{ERM_i} \right)^{2} \right] \quad (9)$$

where W_i is the contamination weight of PTE, C_i is the PTE concentration in the sediment, and n is the number of PTEs used in the analysis. W_i is calculated according to formula 10:

$$W_i = \frac{(loading\ value_i \times eigen\ value)}{\sum_i^n (loading\ value_i \times eigen\ value)} \quad (10)$$

The eigenvalue and load values of the factor/component determined to be anthropogenic are used in the basic components/factor analysis in W_i.

CSI findings are classified as follows: CSI < 0.5 uncontaminated, 0.5 ≤ CSI < 1 very low contaminated, 1 ≤ CSI < 1.5 low severity of contamination, 1.5 ≤ CSI < 2 low to moderate severity of contamination, 2 ≤ CSI < 2.5 moderate severity of contamination, 2.5 ≤ CSI < 3 moderate to high severity of contamination, 3 ≤ CSI < 4 high severity of contamination, 4 ≤ CSI < 5 very high severity of contamination, and CSI ≥ 5 ultra-high severity of contamination.

Calculation of non-carcinogenic health risk indices

The enrichment of PTE with anthropogenic effects in wetlands may pose health risks for humans through the food web depending on the consumption of organisms that feed on sediment such as fish or various methods of exposure. Different risk indices have been developed to analyze health risks. $\mathrm{Exp_{ing}}$ is used to analyze the health risks that arise in the case of ingestion of sediments. $\mathrm{Exp_{derm}}$ is used to analyze the health risks that arise in the case of dermal exposure. In wetlands, direct ingestion of sediments and dermatological exposure are rare. However, PTE stored in the sediment may be released back into the water with the formation of favorable environmental conditions (Yuan et al., 2014). In this case, people may be exposed to dermatological and health risks due to ingestion (drinking) during the supply of drinking water, and utility water from dams that store PTE in their sediment at amounts that may cause ecological and health risks.

$\mathrm{Exp_{ing}}$ is calculated according to formula 11:

$$\mathrm{Exp_{ing}} = \frac{\mathrm{C_{sed}} \times \mathrm{IR} \times \mathrm{UCF} \times \mathrm{EF} \times \mathrm{ED}}{\mathrm{BW} \times \mathrm{AT}} \quad (11)$$

where C_{sed} refers to the PTE concentration, IR is the ingestion rate (114 mg/day), UCF is the unit conversion (10^{-6} mg/kg), EF is the exposure frequency (350 days/year), ED is the exposure duration (assumed as 30 years), BW is the mean body weight (70 kg), and AT shows the average time exposed (30 years × 365 = 10,950 days). According to the formula, it is assumed that a person weighing 70 kg is exposed to 114 mg of PTE per day for 30 years (USEPA, 2002, 2005).

$\mathrm{Exp_{derm}}$ is calculated according to formula 12:

$$\mathrm{Exp_{derm}} = \frac{\mathrm{C_{sed}} \times \mathrm{UCF} \times \mathrm{SA} \times \mathrm{AF} \times \mathrm{ABS} \times \mathrm{EF} \times \mathrm{ED}}{\mathrm{BW} \times \mathrm{AT}} \quad (12)$$

where SA represents the skin area that is exposed (5700 $\mathrm{cm^2}$), AF represents the attachment factor (0.07 $\mathrm{mg/cm^2}$) of the sediment, and ABS refers to the absorption factor of the sediment (0.001) (Song et al., 2019a, b).

HQ and HI are used to detect the non-carcinogenic health risks of PTE by ingestion and dermal exposure. The formula for HQs (hazard quotients) is calculated according to formula 13:

$$\mathrm{HQ_{ing}/HQ_{derm}} = \frac{\mathrm{Exp_{ing}/Exp_{derm}}}{\mathrm{RfD0}} \quad (13)$$

where $\mathrm{Exp_{ing}}$ represents exposure via ingestion, $\mathrm{Exp_{derm}}$ represents dermatological exposure, and RfDO represents the reference dose (USEPA, 2002; Sun & Chen, 2018).

HI (total non-carcinogenic health risks) is calculated according to formula 14:

$$\mathrm{HI} = \sum_{\mathrm{I}=1}^{n} HQ_{ing}/HQ_{derm} \quad (14)$$

A HI value over 1 points to the existence of non-carcinogenic health risks in the wetland, while a value

less than 1 points to no health risks (USEPA, 2002; Sun & Chen, 2018).

Multivariate statistical and spatial analyses

Cluster, factor, and correlation analyses were carried out to determine the common sources and transportation processes of PTE. The findings were transformed into spatial distribution maps by using the kriging interpolation tool in ArcMap 10.7. Kriging interpolation is used to estimate the optimum values of the data at unknown points using known values of nearby points. ArcGIS 10.7 uses formula 15 in kriging interpolation:

$$N_p = \sum_{i=1}^{n} Pi \times Ni \quad (15)$$

where N is the number of sampling points, Ni represents the geoid corrugation values of the points used in the calculation of N_p, N_p is the corrugation value to be calculated, and Pi represents each Ni value used in the calculation of N (ESRI, 2021).

Results and discussion

Spatial distribution of PTEs

According to mean values (ppm), PTE concentration was found as follows: Fe (55.030) > Al (27.220) > Mn (1053) > Cr (181) > Ni (180) > Zn (95) > Cu (62) > As (17) > Pb (11) > Cd (0.20) > Hg (0.108). According to our spatial analysis, minimum concentration for Pb and Hg was observed at station (ST) 8; for Zn, Fe, Ni, and Mn at ST 9; for Cr and Cu at ST 5; for Cd at ST 3; and for As at ST 6. Maximum concentration for Al, Cr, and Ni was observed at ST 8; for Fe, Mn, and Zn at ST 5; for Pb and Cd at ST 1; for As and Cu at ST 11; and for Hg at ST 10. The maximum concentration of As, Hg, and Cu at the mouth of Nilüfer Stream, one of the two important stream tributaries discharged into the dam, indicated that these PTEs were transported from within the basin. The maximum concentration of Fe, Mn, and Zn at the mouth of Kapıkaya Creek showed that these PTEs were discharged from the Kapıkaya Creek basin. It is noteworthy that Al, Cr, and Ni peaked at ST 8, a small seasonal stream inflow passing by the mine, while Pb and Cd peaked near the dam body, where there was no continuous stream inflow but is close to the highway (Fig. 2).

The data obtained from Doğancı dam were compared with the data for PTE concentrations of the dams located in different parts of Turkey and the world (Table 1). According to minimum and maximum concentrations, Al was found to be higher here than all dams except the Manwan Dam. According to the minimum concentration, As was lower here than İkizcetepeler, Manwan, and Castilseras dams and but higher than the other dams. According to the maximum concentration, As was higher here than all the other dams except Manwan Dam. Cd was higher here than all the dams other than the İkizcetepeler Dam, given the minimum concentration, and all the other dams according to the maximum concentration. Cr was higher here than Manwan, Çatören, and Castilseras dams and lower than the other dams in terms of the minimum concentration and higher than all the other dams according to the maximum concentration. Fe was higher here than all the dams other than the Castilseras Dam in terms of minimum concentration, and all the other dams according to the maximum concentration. According to the minimum concentration, Hg was lower than İkizcetepeler Dam and higher than Aguamilpa Dam, while it was higher than both these dams according to the maximum concentration. According to the minimum and maximum concentrations, Pb was lower here than all the dams other than Aguamilpa Dam. Zn was higher here than all the dams except for Castilseras Dam in terms of the minimum concentration, and all the dams other than Manwan Dam according to the maximum concentration (Table 1). The high As, Cd, Cr, Cu, Fe, Hg, Mn, Ni, and Zn concentrations found in Doğancı Dam were noteworthy among the dams randomly selected from the relevant literature. Natural/anthropogenic sources of these PTEs were analyzed with EF, CF, mCd, and I_{geo}.

Spatial distributions of TOC, CDP, and $CaCO_3$

TOC was maximum (4.36%) at ST 10 and minimum (1.20%) at ST 8, with an average of 2.42%. According to the spatial distribution maps, TOC peaked at the mouths of Nilüfer Stream and Kapıkaya Creek

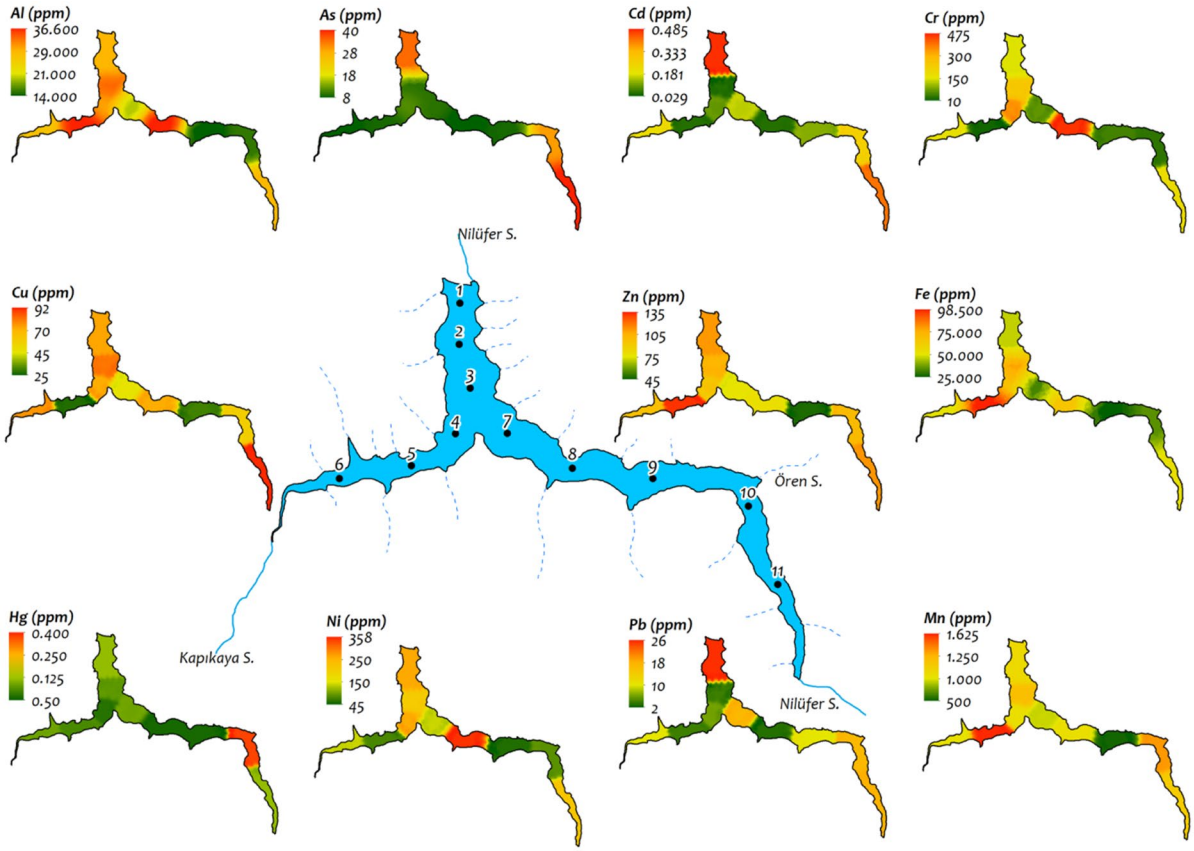

Fig. 2 Spatial distribution of PTEs at the base of the dam in summer of 2019

(Fig. 3). This showed that TOC was discharged from the basin by the rivers, or the primary production increased in these regions depending on the nutrients carried by the rivers. The higher TOC at the mouth of Nilüfer Stream than Kapıkaya Creek indicated the existence of more organic materials in the Nilüfer Stream basin. CDP concentration was minimum (0.44 µg/gr) at ST 9 and maximum (82 µg/gr) at ST 10, with an average of 27 µg/gr. CDP reached a high concentration at the mouths of Nilüfer Stream and Kapıkaya Creek (Fig. 3). The higher CDP concentration at the mouth of Nilüfer Stream suggested that net primary production and/or nutrient inputs into the basin were faster and higher than those into Kapıkaya Creek basin. An increase in Epiphytic algae in Nilüfer Stream due to N and P enrichment was previously reported (Dere et al., 2002; Karaer & Küçükballı, 2006). This in turn showed that the nutrients discharged into the Nilüfer Stream triggered algae growth in the stream and increased the CDP concentration of the dam.

$CaCO_3$ concentration was minimum (0%) at ST 4 and maximum (41.75%) at ST 8, with an average of 8.46%. $CaCO_3$ was discharged by the Kapıkaya Creek, with the seasonal stream located at ST 8 (Fig. 3). There is a limestone formation covering an area of 10.2 km^2 to the south of Kapıkaya Creek and ST 8 (MTA, 2021). Therefore, the source of the high $CaCO_3$ concentration at the mentioned sampling points has lithophyll origin.

Evaluation of PTE contamination with EF, CF, mCd, and I_{geo}

According to the mean EF values, the order of elements was as follows: As (19.96) > Pb (19.81) > Hg (7.13) > Cd (5.22) > Mn (1.25) > Zn (1.09) > Ni (0.93) > Fe (0.90) > Cu (0.87) > Cr (0.65). As, Cd, Hg, and Pb were significantly

Table 1 Comparison of PTE concentrations between this study and other dams

Location		Al	As	Cd	Cr	Cu	Fe	Hg	Mn	Ni	Pb	Zn
Doğancı Dam (Turkey)												
(This study)	**Min**	14300	7.90	0.07	22.50	28.03	25200	0.017	575	59.80	2.83	47.01
	Max	36600	39.94	0.47	455.20	89.99	95800	0.361	1603	345.60	25.04	131.10
	Std.	7190	12.76	0.14	143.07	20.58	22190	0.09	279	94.18	7.75	23.24
İkizcetepeler Dam (Turkey)												
(Fural et al., 2020)	**Min**	10170	16.60	0.09	12.80	10.60	20000	0.025	402	16.50	14.68	33.45
	Max	20520	32.90	0.19	30	22.20	30020	0.108	1.159	54.70	36.56	65.65
Manwan Dam (China)												
(Wang et al., 2012)	**Min**	24500	10.30		38.29	15.85	19100		246.58		17.03	45.32
	Max	61000	72.56		89.85	56.32	37900		769.06		92.20	259.84
Çatören Dam (Turkey)												
(Çiftçi, 2015)	**Min**	3500	0.001		30.15	18.50			112	7.50	12.50	19.23
	Max	13000	0.01		140.70	42.20			425	38.25	26.83	42.41
Aguamilpa Dam (Mexico)												
(Peraza et al., 2015)	**Min**	7760		0.01	0.22	0.79	4740	0.01		0.24		14.80
	Max	27600		0.27	18.30	60.80	15900	0.04		189	13.06	54.88
Castilseras Dam (Spain)												
(Ordiales et al., 2015)	**Min**	10400	8.32		52.69	7.45	30050		433	27.74	20.95	65.61
	Max	15800	14.30		85.69	21.51	51700		666	60.31	50.84	116.82

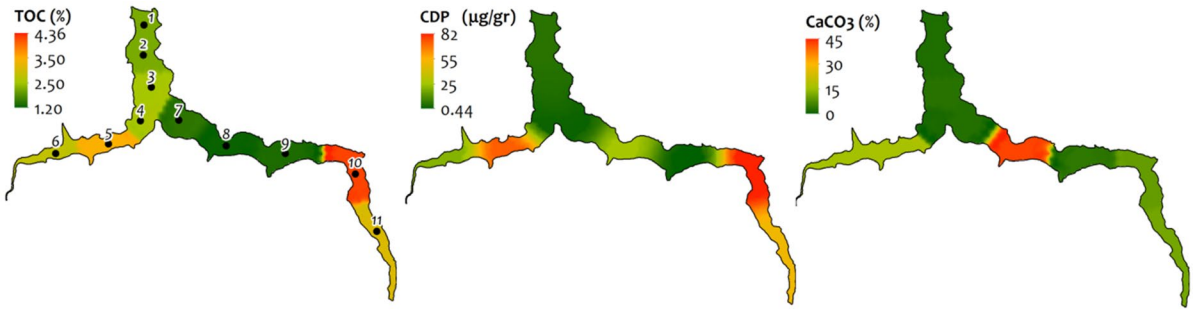

Fig. 3 Spatial distribution of TOC, CDP, and $CaCO_3$ in summer of 2019

enriched by exposure to various anthropogenic effects. No anthropogenic effects were detected for Mn, Zn, Ni, Fe, Cu, and Cr. Based on the mean CF data, the order of elements was as follows: Pb (29) > As (24) > Hg (7) > Cd (6) > Mn (1.66) > Zn (1.46) > Al (1.41) > Ni (1.34) > Cu (1.17) > Cr (0.98). As, Cd, Hg, and Pb were at their peak contamination levels. The other PTEs were of low contamination; that is, they were of natural origin.

mCd was minimum (3.15) at ST 8 and maximum (13.54) at ST 1, with an average of 7.07. Contamination was detected in the lower limits of high degrees of contamination based on mCd. According to the spatial analyses, the mCd values (12 +) at the mouth of Nilüfer Stream and near the dam body were noteworthy. The source of high mCd was indicative of very high contamination of As, Cd, Hg, and Pb. Nilüfer Stream discharged more anthropogenic PTE than did Kapıkaya Creek (Fig. 2). Some previous studies confirmed that Nilüfer Stream discharged organic and inorganic pollutants into Doğancı Dam (Dere et al., 2002; Karaer & Küçükballı, 2006; Güleryüz et al., 2008; Üstün, 2011). The highest mCd value occurred with ST 1 near the dam body, which does not have a stream entrance. The possible sources of Pb and Cd, which caused very high mCd values at this point, were the highway passing over the dam body, because transportation networks close to wetlands can increase Pb and Cd concentrations up to 320 m (Viard et al., 2004). This was supported considering that ST 1 was located 120 m away from the dam body, whose Pb and Cd concentrations were at the maximum level. The likely source of As and Cd reaching high concentrations and contamination levels at the mouth of the Nilüfer Stream was agriculture, because 24.50% (110.41 km^2) of the basin is agricultural land. Cd is the raw material of inorganic fertilizers frequently used in agriculture (Chen et al., 2021), while As is a raw material used in pesticides and herbicides (Acquavita et al., 2021).

The Hg concentration peaked at the mouth of the Nilüfer Stream and was of anthropogenic origin. The natural concentration level of Hg due to the weathering of volcanic rocks rose due to industrial activities such as mines (Baumann et al., 2019). Our spatial analysis showed no anthropogenic activity such as mining near ST 10, where Hg peaked. However, industrial and domestic wastewater in the Nilüfer Stream basin was carried by the river and discharged to the dam (Karaer & Küçükballı, 2006) as the main anthropogenic sources of Hg (Jahan & Strezov, 2018; Song et al., 2019a, b).

According to the mean I_{geo} values, the elements were listed as follows: As (3.75) > Pb (3.59) > Hg (1.94) > Cd 1.79 > Mn (0.10) > Zn (−08) > Al (−0.16) > Fe (−0.32) > Ni (−0.36) > Cu (−0.45) > Cr (−1.13). The base of the dam was exposed to anthropogenic effects with Pb and As severely, with Hg and Cd moderately, and uncontaminated with Mn or contaminated moderately. No anthropogenic effects were detected for Zn, Al, Fe, Ni, Cu, and Cr. The indices calculated for the identification of PTE sources indicated that As, Pb, Cd, and Hg were of anthropogenic origin, whereas Al, Cr, Cu, Fe, Ni, Mn, and Zn were of natural origin (Fig. 4).

Toxicological risk assessment with TRI

TRI was maximum (22) at ST 8 and minimum (5) at ST 9, with an average of 13.51. A moderate toxic risk existed throughout the dam. The local anthropogenic effects created considerable toxic risks at ST 1, 2, 4, and 11 and caused a very high toxic risk at ST 8

(Fig. 5). The order of responsibility of PTEs for toxic risk was as follows: Ni (45.89%) > Cr (23.53%) > Cu (10.58%) > As (9.69%) > Zn (4.29%) > Hg (3.18%) > Pb (1.70%) > Cd (1.14%). The fact that TRI peaked at a seasonal river mouth that discharges to ST 8 instead of the main river mouths feeding the dam pointed to an anthropogenic effect at this point. However, Ni (45.89%) and Cr (23.53%) are responsible for the very high toxic risk at ST 8. Ni and Cr are released into nature by the decomposition of rocks of volcanic origin (Kelepertzis et al., 2013). Our literature, spatial, and statistical analyses and findings verified that Ni and Cr were discharged into the dam by seasonal streams and emerged during the decomposition of metaclastic rocks of volcanic origin located to the south of ST 8. The source of the considerable toxic risk at ST 4 was related to the release of Ni and Cr into nature due to the decomposition of volcanic rocks, as was the case at ST 8. The highway was the probable source of the considerable toxic risk at ST 1 and 2, located near the dam body and with no stream discharge. Cu (10.58%), As (9.69%), and Zn (4.29%) were responsible for the considerable toxic risk at ST 11 at the mouth of Nilüfer Stream. The possible source of Cu, As, and Zn was the agricultural activities carried out in the basin (Acquavita et al., 2021; Chen et al., 2021; Wei et al., 2007).

Ecological risk assessment with CSI, mHQ, and ECI

CSI was minimum (0.48) at ST 9 and maximum (5.52) at ST 8, with an average of 2.31 (moderately contaminated). However, some strong local anthropogenic effects caused an ultra-high severity of contamination at ST 8 and a high severity of contamination at ST 1, 2, 4, and 11. The order of responsibility for PTEs for the total contamination was as follows: Ni (80.51%) > As (7.37%) > Cu (5.26%) > Cr (2.97%) > Zn (2.41%) > Hg (0.55%) > Cd (0.50%) > Pb (0.43%). The reason for CSI peaking at ST 8 was the lithological Ni release. Lithogenic Ni and Cr releases and anthropogenic As, Cu, and Zn were effective in detecting the moderate contamination throughout the dam.

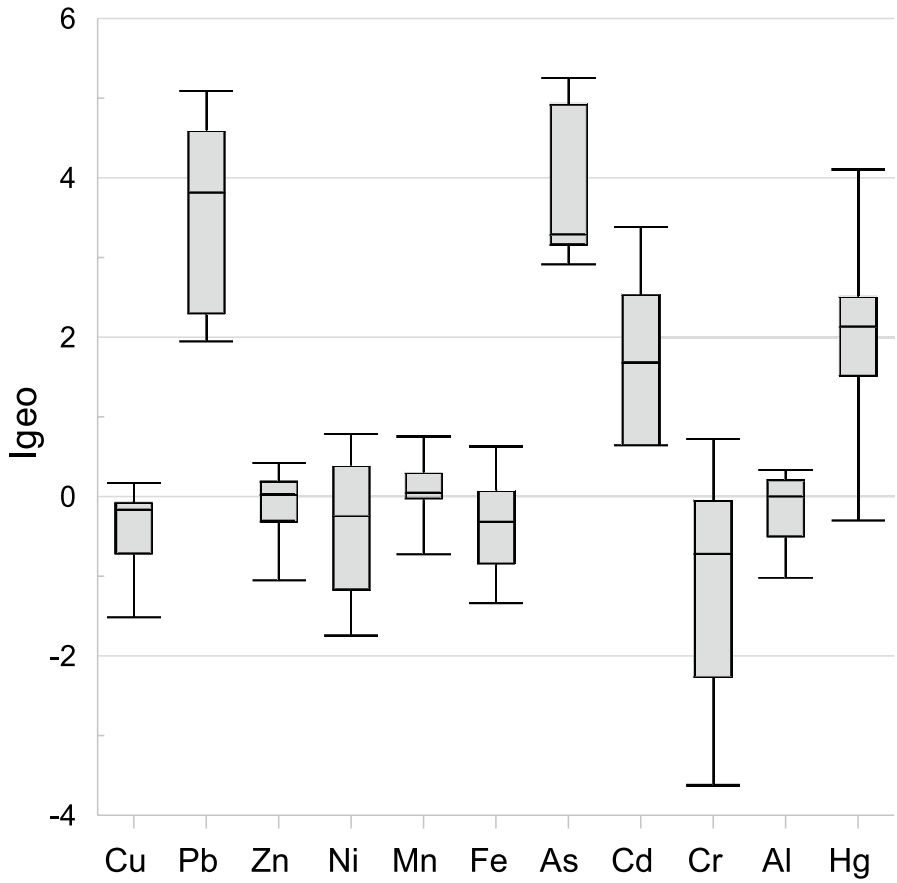

Fig. 4 Box whisker diagram of I_{geo}

According to the average mHQ values, the elements were listed as follows: Ni (4.04) > Cr (2.70) > As (2.01) > Cu (1.60) > Zn (1.09) > Hg (0.88) > Pb (0.66) > Cd (0.60). Ecological risk exhibited extreme severity for Ni, high severity for Cr, considerable severity for As, and moderate severity for Cu. Severity level was low for Zn and very low for Hg, Pb, and Cd. The maximum mHQ values were determined for Cu and As at ST 11, for Pb and Cd at ST 1, for Ni and Cr at ST 8, for Zn at ST 5, and for Hg at ST 10. Ni (5.78) and Cr (4.63) mHQ values were at the maximum level at the mouth of the seasonal stream passing near the mine and discharged to ST 8 (Fig. 5). Being released into nature by volcanic origin magmatic and metamagmatic rock weathering, Ni and Cr led to PTE enrichment in water and sediment (Kelepertzis et al., 2013). There are metaclastic rock formations to the south of ST 8, where Ni and Cr mHQ levels peaked (MTA, 2021). Since marble, which consists of rocks of sedimentary origin, is mined near ST 8, anthropogenic intervention cannot be applied to the volcanic rocks. Therefore, the possible sources of Ni and Cr were lithogenic factors. Our findings confirmed that Ni and Cr together with Al, Fe, and Mn were of lithogenic origin. The fact that the mHQ level of Cr was above 3 at ST 11 at the mouth of the Nilüfer Stream was related to the discharge of Cr into the dam by the stream, which is released into nature by the decomposition of the volcanic rocks in the Nilüfer Stream basin. High Cr concentration was detected in water samples in a study conducted to determine the water quality of Nilüfer Stream (Üstün, 2011).

mHQ values for As were 3.02 at ST 1 near the highway on the dam body and maximum (3.21) at ST 10 at the mouth of Nilüfer Stream. As was affected by the highway and agricultural activities in the Nilüfer Stream basin. Cu peaked (1.95) at ST 10 at the mouth of the Nilüfer Stream. The probable source of Cu, which reached 1.75 at the mouth of Kapıkaya Creek, was agricultural activities in the basin because Cu

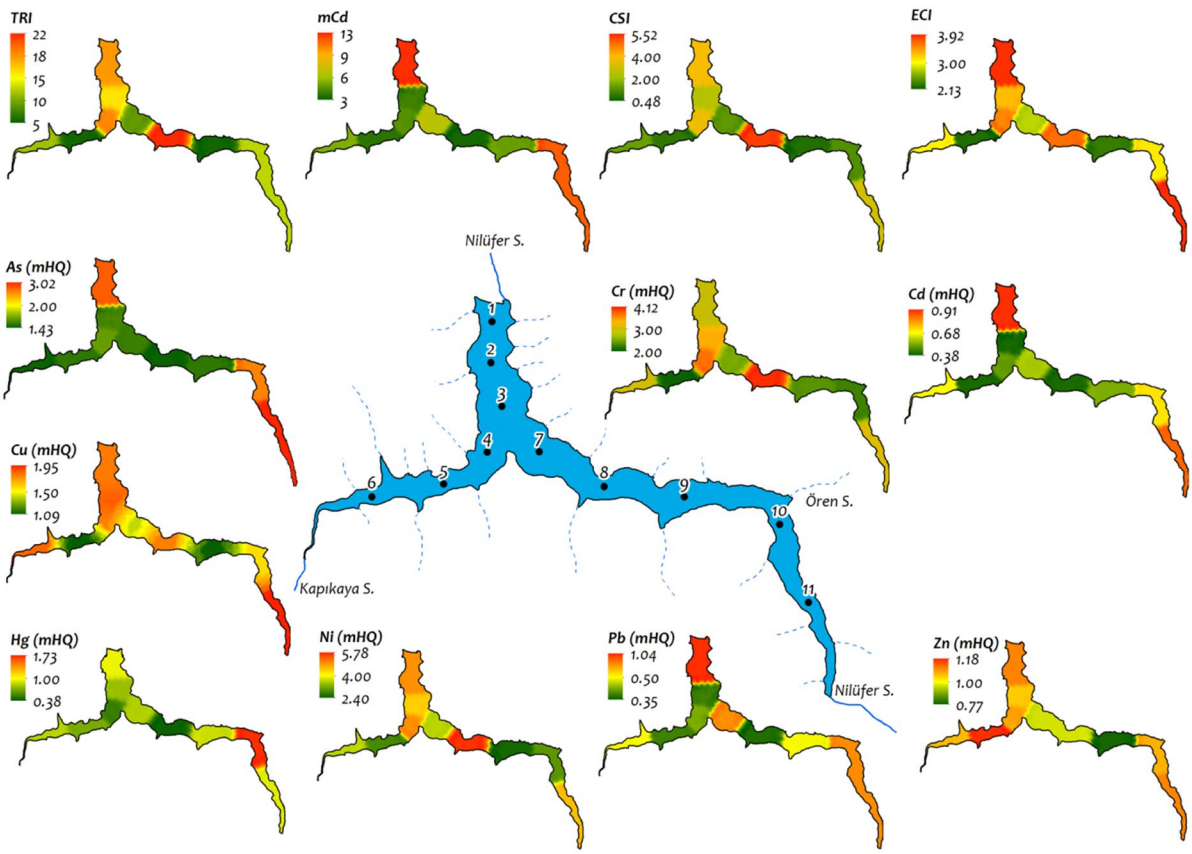

Fig. 5 Spatial analysis of TRI, mCd, CSI, ECI, and mHQ in summer of 2019

along with Zn and Cd are among the raw materials of inorganic fertilizers used in agriculture (Chen et al., 2021; Wei et al., 2007). Our spatial and statistical analyses confirmed the common origin of Cu, Zn, and Cd. However, since Cd is of dual origin, including agriculture and the highway, it was included in the same cluster with Pb and As in the cluster analysis.

In PTE analyses conducted on some plant species in Nilüfer Stream, it was determined that Cr, Cu, Ni, and Zn reached high concentrations (Güleryüz et al., 2008). This showed that Nilüfer Stream discharged Cr, Cu, Ni, and Zn into the dam. The findings of past years overlapped with the PTE concentration and spatial analyses of the sediment samples taken in this study from the sampling points at the mouth of the Nilüfer Stream. No source identification was made for PTEs with low, very low, and insignificant mHQ levels.

ECI was maximum (3.92) at ST 11 and minimum (2.13) at ST 5. It was uncontaminated to slightly contaminated at ST 5, 7, and 9 and slightly to moderately contaminated at all the other points. The mean ECI of 3.14 pointed to a slight-to-moderate contamination across the base of the dam. The reason for ECI peaking at ST 11 was the mHQ levels of Cu, As, and Zn from agricultural activities and the mHQ levels of the lithogenic Ni and Cr. The ECI (3.88) level at ST 1, close to the highway on the dam body, resulted from the mHQ level of Pb, Cd, and As. In the spatial analysis, no anthropogenic effect was detected at ST 1, except for the highway (Fig. 5).

Non-carcinogenic health risk assessment with HI

According to the mean HI values, the elements were listed as follows: Fe (0.1232) > Cr (0.0949) > As (0.0910) > Al (0.0427) > Ni (0.0257) > Mn (0.0118) > Pb (0.0051) > Cu (0.0024) > Hg (0.0006) > Zn (0.0005) > Cd (0.0003). Thus, no PTE in the dam caused non-carcinogenic health problems.

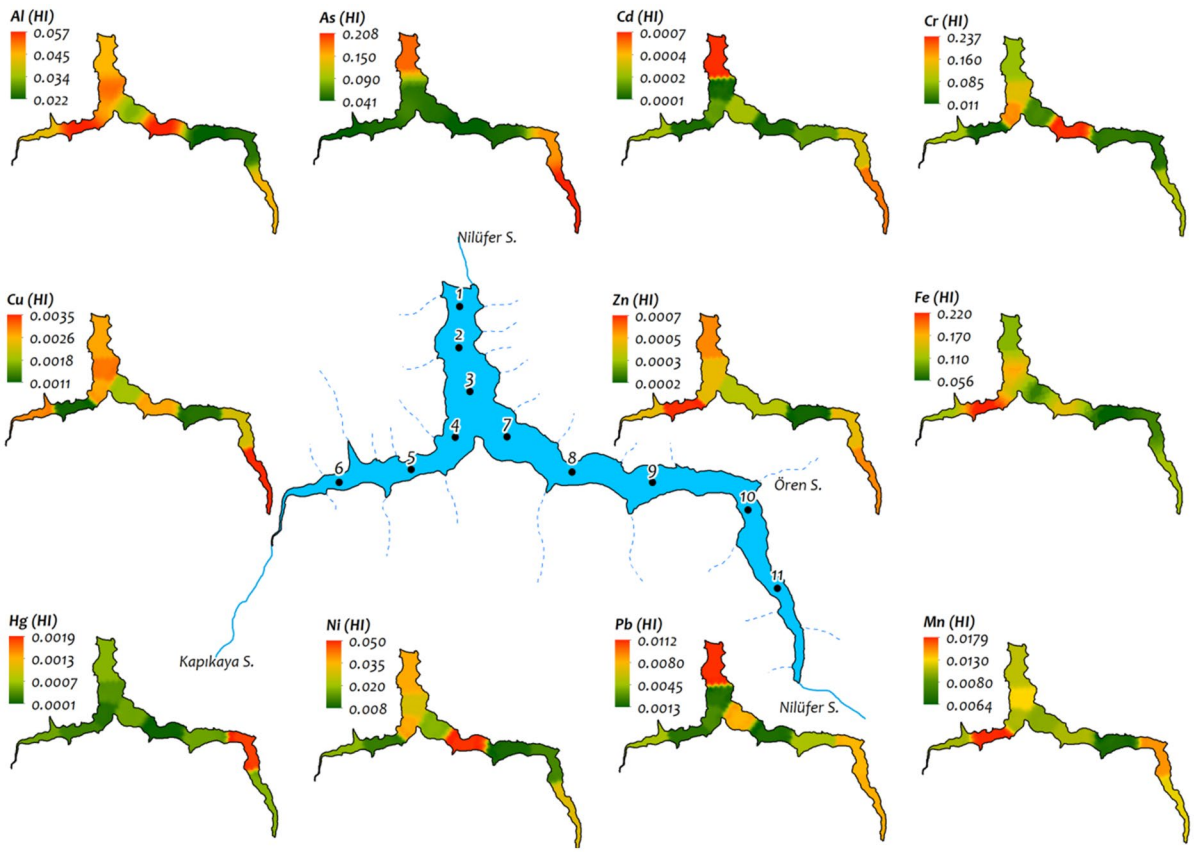

Fig. 6 Spatial analysis of HI in summer of 2019

Currently, there is no health risk in the dam sediments. However, the sampling points with maximum HI should be monitored in future studies. The maximum HI values according to the stations are as follows: Al ST 8 (0.0574), As ST 11 (0.2084), Cd ST 1 (0.0007), Cr ST 8 (0.2378), Cu ST 11 (0.0035), Zn ST 5 (0.0007), Fe ST 5 (0.2205), Hg ST 10 (0.0019, Ni ST 8 (0.0492), Pb ST 1 (0.0112), and Mn ST 5 (0.0179). Thus, the PTEs closest to the health risk limit (1) were As, Cr, and Fe. The source of Cr and Fe was lithogenic, while the source of As was anthropogenic. Our PCA and Cluster analyses also supported these findings. Spatial analyses confirmed that As peaked at the mouth of the Nilüfer Stream, which should be carefully monitored in future studies. The probable source of As at the mouth of the Nilüfer Stream was herbicides and pesticides used in agriculture in the basin. The water quality of the Nilüfer Stream is steadily declining (Üstün, 2011), and hence, more serious and effective measures should be taken against anthropogenic effects such as agriculture and domestic and industrial wastewater in the Nilüfer Stream basin (Fig. 6).

Multivariate statistical analyses

According to Spearman correlation analysis, Cu had a positive relationship with Pb, Zn, Ni, Fe, As, Cd, and Cr but a negative one with TOC. Pb had a very strong positive correlation with As, Cd, Hg; a strong negative one with Fe and Al; and a negative one with Cr, TOC, and $CaCO_3$. The strong negative correlation between Pb and the lithophile PTEs of Al and Fe supported the finding that Pb was influenced by anthropogenic sources. Zn showed positive correlations with Mn, Fe, Al, As, Hg, and CDP. Ni had a positive correlation with Fe, As, Cr, and Al but a negative one with Hg and TOC. Mn had a positive correlation with Fe, As, Al, TOC, and CDP but a negative one with Cr. Fe exhibited a strong negative correlation with Cd, Hg, and Pb and a negative one with As. The negative correlation between the PTEs, exposed to the most anthropogenic effects in the dam, and Fe, a lithophile PTE, was evidence of an anthropogenic effect. Fe was positively correlated with Al, Cr, TOC, CDP, and $CaCO_3$, while As had a strong positive correlation with Cd, Hg, and Pb (Table 2). This was another important indicator that As, Cd, Hg, and Pb were exposed to anthropogenic effects.

Table 2 Spearman correlation analysis matrix

PTE	Cu	Pb	Zn	Ni	Mn	Fe	As	Cd	Cr	Al	Hg	TOC	CDP	$CaCO_3$
Cu														
Pb	**0.248**													
Zn	**0.333**	0.139												
Ni	**0.551**	−0.006	0.066											
Mn	0.115	−0.054	**0.854**	−0.018										
Fe	**0.236**	**−0.648**	**0.575**	**0.284**	**0.612**									
As	**0.401**	**0.699**	**0.516**	**0.261**	**0.486**	−0.018								
Cd	**0.337**	**0.951**	0.177	0.067	−0.067	**−0.595**	**0.590**							
Cr	**0.648**	**−0.309**	−0.175	**0.806**	**−0.212**	**0.369**	−0.042	**−0.227**						
Al	0.163	**−0.660**	**0.406**	**0.563**	**0.418**	**0.878**	−0.127	**−0.595**	**0.503**					
Hg	0.163	**0.890**	**0.212**	**−0.284**	0.103	**−0.636**	**0.547**	**0.865**	**−0.503**	**−0.721**				
TOC	**−0.648**	**−0.333**	−0.042	**−0.345**	**0.284**	**0.224**	0.012	**−0.509**	**−0.369**	0.103	**−0.369**			
CDP	0.078	−0.018	**0.672**	−0.006	**0.745**	**0.357**	0.194	0.128	**−0.200**	**0.272**	0.187	−0.042		
$CaCO_3$	−0.127	**−0.442**	0.187	−0.187	0.175	**0.248**	**−0.516**	**−0.276**	−0.078	**0.272**	−0.187	−0.163	**0.636**	

Bold expressions indicate significant correlations at 95% confidence interval

Table 3 Weight of principal components

PTE	Component 1	Component 2	Component 3	Component 4
Cu	0.075	**0.303**	−0.384	0.009
Pb	−0.388	**0.157**	−0.178	−0.112
Zn	0.068	**0.464**	0.193	−0.271
Ni	**0.255**	0.181	−0.370	0.003
Mn	0.071	0.361	**0.395**	−0.036
Fe	**0.360**	0.204	0.240	−0.223
As	−0.275	**0.374**	−0.116	−0.033
Cd	−0.297	**0.312**	−0.241	−0.092
Cr	**0.338**	0.050	−0.323	0.125
Al	**0.393**	0.254	−0.002	−0.149
Hg	−0.358	0.137	0.146	**0.290**
TOC	0.045	−0.187	**0.328**	−0.209
CDP	−0.078	0.308	0.353	**0.430**
$CaCO_3$	0.250	0.084	−0.008	**0.707**

Our PCA showed four components with an eigenvalue > 1, explaining 88.97% of the total variance. Component 1 consisted of Ni, Fe, Cr, and Al. According to the findings, component 1 was of lithological origin. Component 2 consisted of Cu (which created a medium ecological risk according to the mHQ data), Zn (which created an ecological risk at the upper limits of low levels), and Cd, Pb, and As (which were enriched with anthropogenic effects). In this case, component 2 consisted of the PTEs of anthropogenic origin. Component 3 consisted of Mn, a lithophile PTE, and TOC. Component 4 included CDP (discharged from the basin into the dam by rivers), $CaCO_3$ of lithogenic origin and Hg of anthropogenic origin (transported from the basin by the Nilüfer Stream). Component 4 was of lithological and anthropogenic origins with common transport processes (Table 3).

According to the cluster analysis, Cu, Ni, Cr, Zn, Mn, Fe, Al, and CDP were in the same cluster. This cluster consisted of the lithophilic PTEs and CDP. Pb, Cd, and As were exposed to anthropogenic effects and located in the same cluster, while Hg was in a closely related cluster. This in turn supported that Pb, Cd,

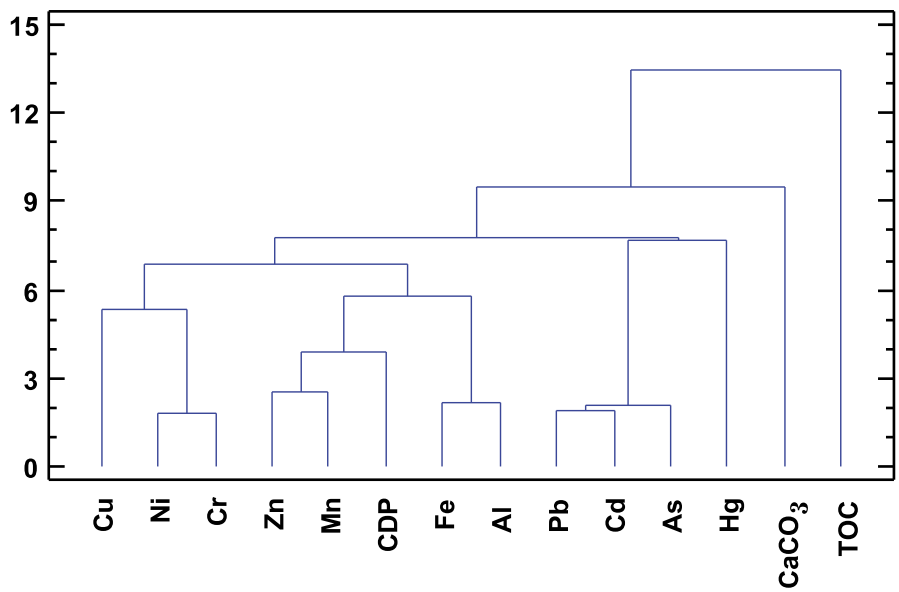

Fig. 7 Cluster analysis

As, and Hg were of anthropogenic origin. Although $CaCO_3$ and TOC were in different clusters, they were associated with the lithophile-based PTEs. The presence of carbonate rocks in the basin also confirmed that $CaCO_3$ was of lithophilic origin (Fig. 7).

Conclusion

Based on our findings, As, Pb, Cd, and Hg were defined as the PTEs of anthropogenic origin. Ni and Cr were determined to be of lithological origin. As was affected by agriculture and transportation networks, while Cu was affected only by agriculture. These elements created a moderate level of toxic risk throughout the dam and caused a considerable-to-very high toxic risk at some sampling points. CSI data showed a moderate PTE contamination in the dam. According to the mHQ value, ecological risk was identified at extreme severity for lithological Ni, high severity for Cr, considerable severity for anthropogenic As, and moderate severity for Cu. The ECI value pointed to a slight-to-moderate contamination across the dam. The HI value demonstrated no non-carcinogenic health risks in the dam. Our spatial analyses showed that the PTEs became more enriched near the mouth of the Nilüfer Stream and the dam body than the other sampling points, thus creating ecological and health risks. Overall, a moderate level PTE contamination, a moderate ecological risk, and a very low level of non-carcinogenic health risk existed in Doğancı Dam due to natural factors and anthropogenic activities. It is crucial to continue monitoring the highway near the dam body, mining activities south of the dam, and the other human disturbances such as agriculture and wastewater in the Nilüfer Stream basin, based on the ecological and health risk level of the PTEs. To minimize ecological deterioration and health risks,

- The ecological effects of the highway on the dam body should be analyzed with a more specific focus.
- Environmental impact audits should be carried out in the mines to the south of the dam and the factories in the basin.
- The use of chemical fertilizers in agricultural activities should be restricted. Organic farming should be encouraged in the basin.
- Strict measures should be taken to prevent the wastewater of settlements from being discharged into the Nilüfer Stream and Kapıkaya Stream.

Acknowledgements We would like to thank Prof. Dr. A. Evren Erginal for his contributions to developing the project, and Bursa Metropolitan Municipality General Directorate of Water and Sewerage Administration, and Prof. Dr. Abdulah Soykan and Furkan İnan for their support in the field work conducted in this project.

Author contribution Ş.F.: conceptualization, methodology, software, data curation, investigation, writing — original draft, visualization. S.K.: conceptualization, methodology, formal analysis, writing – original draft, writing — review & editing. İ.C.: conceptualization, funding acquisition, project administration, resources, writing — review & editing. D.A.: conceptualization, investigation, validation, writing – original draft, writing — review & editing. All authors read and approved the final manuscript.

Funding This study was supported by Balıkesir University Scientific Research Projects Unit (BAP) within the scope of the project coded SB 2019–030.

Availability of data and materials The datasets used and/or analyzed during the current study are available from the corresponding author on reasonable request via e-mail.

Declarations

Ethical approval Not applicable.

Consent to participate Not applicable.

Consent for publication All authors approve the publication of the article in your journal.

Competing interests The authors declare no competing interests.

References

Abrahim, G., & Parker, R. (2008). Assessment of heavy metal enrichment factors and the degree of contamination in marine sediments from Tamaki Estuary, Auckland. *New Zealand. Environmental Monitoring and Assessment, 136*, 227–238.

Acquavita, A., Floreani, F., & Covelli, S. (2021). Occurrence and speciation of arsenic and mercury in alluvial and coastal sediments. *Current Opinion in Environmental Science & Health*. https://doi.org/10.1016/j.coesh.2021.100272

Aydın, O., Ünaldı, Ü. E., Duman, N., Çiçek, İ, & Türkoğlu, N. (2017). Evaluation of water scarcity in Turkey at a spatial scale. *Turkish Journal of Geography, 68*, 11–18.

Baumann, Z., Jonsson, S., Mason, R. P. (2019). Geochemistry of mercury in the marine environment. In Encyclopedia of ocean sciences (third edition). Edited by Cochran JK, Bokuniewicz HJ, Yager PL. *Academic Press*, 301–308.

Benson, N. U., Adedapo, A. E., Fred-Ahmadu, O. H., Williams, A. B., Udosen, E. D., Ayejuyo, O. O., & Olajire, A. A. (2018). A new method for assessment of sediment-associated contamination risks using multivariate statistical approach. *MethodsX, 5*, 268–276. https://doi.org/10.1016/j.mex.2018.03.005

Bursa Metropolitan Municipality Water and Sewerage Administration (BUSKI). (2021). https://www.buski.gov.tr/tr/icerik/doganci_baraji_565. Accessed 21 Jun 2021.

Chakraborty, B., Bera, B., Roy, S., et al. (2021). Assessment of non-carcinogenic health risk of heavy metal pollution: Evidences from coal mining region of eastern India. *Environmental Science and Pollution Research, 28*, 47275–47293. https://doi.org/10.1007/s11356-021-14012-3

Chen, Z., Huang, B., Hu, W., et al. (2021). Ecological-health risks assessment and source identification of heavy metals in typical greenhouse vegetable production systems in Northwest China. *Environmental Science and Pollution Research, 28*, 42583–42595. https://doi.org/10.1007/s11356-021-13679-y

Coordination of Information on the Environment (CORINE). (2018). https://land.copernicus.eu/pan-european/corine-land-cover. Accessed 05 Feb 2021.

Çiftçi, M. (2015). Determination of Seydisuyu basin (Eskişehir) water and sediment quality. Anadolu University Graduate School of Science, Master Thesis.

Dere, Ş, Karacaoğlu, D., & Dalkıran, N. (2002). A study on the epiphytic algae of the Nilüfer Stream (Bursa). *Turkish Journal of Botany, 26*(4), 219–233.

El-Alfy, M. A., Dina, H., Darwish, D. H., & El-Amier, Y. A. (2021). Land use Land cover of the Burullus Lake shoreline (Egypt) and health risk assessment of metal-contaminated sediments. *Human and Ecological Risk Assessment: An International Journal*, *27*(4), 898-920, https://doi.org/10.1080/10807039.2020.1786667

Elsagh, A., Jalilian, H., & Aslshabestari, M. G. (2021). Evaluation of heavy metal pollution in coastal sediments of Bandar Abbas, the Persian Gulf, Iran: Mercury pollution and environmental geochemical indices. *Marine Pollution Bulletin, 167*, 112314. https://doi.org/10.1016/j.marpolbul.2021.112314

ESRI. (2021). https://desktop.arcgis.com/en/arcmap/10.3/tools/3d-analyst-toolbox/how-kriging-works.htm. Accessed 14 Feb 2021.

Food and Agriculture Organization of the United Nations (FAO). (2007). The State Of Food And Agriculture. Rome, Italy: World Wildlife Fund. http://www.fao.org/3/a1200e/a1200e.pdf. Accessed 19 May 2021.

Falkenmark, M., Lundqvist, J., & Widstrand, C. (1989). Macro-scale water scarcity requires micro-scale approaches. *Natural Resources Forum, 13*, 258–267.

Farsani, M. N., Haghparast, J. R., Naserabad, S. S., Moghadas, F., Bagheri, T., & Gerami, M. H. (2019). Seasonal heavy metal monitoring of water, sediment and common carp (Cyprinus carpio) in Aras Dam Lake of Iran. *International Journal of Aquatic Biology, 7*(3).

Fural, Ş., Kükrer, S., Cürebal, I. (2020). Geographical information systems based ecological risk analysis of metal accumulation in sediments of İkizcetepeler Dam Lake (Turkey). *Ecological Indicators, 119*. https://doi.org/10.1016/j.ecolind.2020.106784

Fural, Ş., Kükrer, S., Cürebal, İ., & Aykır, D. (2021). Spatial distribution, environmental risk assessment, and source identification of potentially toxic metals in Atikhisar dam, Turkey. *Environmental Monitoring and Assessment, 193*(5), 268. https://doi.org/10.1007/s10661-021-09062-6

Ftrstner, U. (1976). Lake sediments as indicators of heavy-metal pollution. *Naturwissenschaften, 63*, 463–470.

Gaudette, H., Flight, W., Toner, L., & Folger, D. (1974). An inexpensive titration method for the determination of organic carbon in recent sediments. *Journal of Sedimentary Research., 44*, 249–253.

Güleryüz, G., Arslan, H., Çelik, C., Güçer S., Kendall, M. (2008). Heavy metal content of plant species along nilüfer stream in industrialized Bursa City, Turkey. *Water Air Soil Pollution, 195*, 275 - 284. https://doi.org/10.1007/s11270-008-9745-5

Hakanson, L. (1980). An ecological risk index for aquatic pollution control: A sedimentological approach. *Water Research, 8*(14), 975–1001.

Haghshenas, V., Kafaei, R., Tahmasebi, R., et al. (2020). Potential of green/brown algae for monitoring of metal(loid)s pollution in the coastal seawater and sediments of the Persian Gulf: Ecological and health risk assessment. *Environmental Science and Pollution Research, 27*, 7463–7475. https://doi.org/10.1007/s11356-019-07481-0

Hu, C., Yang, X., Dong, J., & Zhang, X. (2018). Heavy metal concentrations and chemical fractions in sediment from Swan Lagoon, China: Their relation to the physiochemical properties of sediment. *Chemosphere, 209*, 848–856.

Jahan, S., & Strezov, V. (2018). Comparison of pollution indices for the assessment of heavy metals in the sediments of seaports of NSW, Australia. *Marine Pollution Bulletin, 128*, 298–306. https://doi.org/10.1016/j.marpolbul.2018.01.036

Karaer, F., & Küçükballı, A. (2006). Monitoring and water quality and assessment of organic pollution load in the Nilüfer Stream, Bursa. *Environmental Monitoring and Assessment, 114*, 391 - 417. https://doi.org/10.1007/s10661-006-5029-y

Kelepertzis, E., Galanos, E., & Ioannis, M. (2013). Origin, mineral speciation and geochemical baseline mapping of Ni and Cr in agricultural topsoils of Thiva Valley (central Greece). *Journal of Geochemical Exploration, 125*, 56–68. https://doi.org/10.1016/j.gexplo.2012.11.007

Kükrer, S., Erginal, A. E., Kılıç, Ş., Bay, Ö., Akarsu, T., & Öztura, E. (2020). Ecological risk assessment of surface sediments of Çardak Lagoon along a human disturbance gradient. *Environmental Monitoring and Assessment, 192*(6), 359. https://doi.org/10.1007/s10661-020-08336-9

Lorenzana, M. R., Yeow, Y. A., Colman, J. T., ChaPpell, L. L., & Choudhury, H. (2008). Arsenic in seafood: Speciation issues for human health risk assessment. *Human and Ecological Risk Assessment: An International Journal, 15*(1), 185–200.

Long, E., Field, L., & Mac Donald, D. (1998). Predicting toxicity in marine sediments with numerical sediment quality

guidelines. *Environmental Toxicology and Chemistry, 17*, 714–727.

Lorenzen, C. (1971). Chlorophyll-degradation products in sediments of Black Sea. *Woods Hole Oceanographic Institution Contribution, 28*, 426–428.

Lu, J., Lu, H., Lei, K., et al. (2019). Trace metal element pollution of soil and water resources caused by small-scale metallic ore mining activities: A case study from a sphalerite mine in North China. *Environmental Science and Pollution Reseach, 26*, 24630–24644. https://doi.org/10.1007/s11356-019-05703-z

Luczynskaa, Z., & Kang, M. (2018). Risk assessment of toxic metals in marine sediments from the Arctic Ocean using a modified BCR sequential extraction procedure. *Environ. Sci. Health, 53*, 278–293. https://doi.org/10.1080/10934529.2017.1397443

MacDonald, D. D., Carr, R. S., & Calder, F. D. (1997). Development and evaluation of sediment quality guidelines for Florida coastal waters. *Oceanographic Literature Review, 6*, 638.

MacDonald, D. D., Ingersoll, C. G., & Berger, T. A. (2000). Development and evaluation of consensus-based sediment quality guidelines for freshwater ecosystems. *Archives of Environmental Contamination and Toxicology, 39*, 20–31. https://doi.org/10.1007/s002440010075

Magni, L. F., Castro, N. L., & Rendina, A. E. (2021). Evaluation of heavy metal contamination levels in river sediments and their risk to human health in urban areas: A case study in the Matanza-Riachuelo Basin, Argentina. *Environmental Research, 197*.

Marzio, A. D., Lambertucci, S. A., Fernandez, A. G., & Lopez, M. E. (2019). From Mexico to the Beagle Channel: A review of metal and metalloid pollution studies on wildlife species in Latin America. *Environmental Research, 176*.

Müller, G. (1969). Index of geoaccumulation in sediments of the Rhine River. *Geo Journal, 2*, 108–118.

Mineral Research and Exploration Department (MTA). (2021). http://earthsciences.mta.gov.tr/mainpage.aspx. Accessed 18 Mar 2021.

Nargis, A., Rashid, H. O., Jhumur, A. K., Haque, M. E., Islam, M. N., Habib, A., et al. (2019). Human health risk assessment of toxic elements in fish species collected from the river Buriganga, Bangladesh. *Human and Ecological Risk Assessment: An International Journal, 26*(1), 120–146.

Niu, Y., Jiang, X., Wang, K., Xia, J., & Jiao, W. (2020). Meta analysis of heavy metal pollution and sources in surface sediments of Lake Taihu, China. *Science of The Total Environment, 700*(134509).

Ordiales, E., Esbrí, J., Covelli, S., Berdonces, M., Higueras, P., Loredo, J. (2015). Heavy metal contamination in sediments of an artificial reservoir impacted by long-term mining activity in the Almadén mercury district (Spain). *Environmental Science and Pollution Research, 23*(7). https://doi.org/10.1007/s11356-015-4770-6

Peraza, J., Anda, J., Farias, F., & Rode, M. (2015). Assesment of heavy metals in sediments of Aguamilpa Dam. *Mexico. Environmental Monitoring and Assessment, 3*(187), 4359–4370. https://doi.org/10.1007/s10661-015-4359-z

Pejman, A., Bidhendi, N. G., Ardestani, M., Saeedi, M., & Baghvand, A. (2015). A new index for assesing heavy metal contamination in sediments: A cese study. *Ecological Indicators, 58*, 365–373.

Schlicting, E., & Blume, E. (1966). *Bodenkundliches Praktikum*. Hamburg und Berlin.: Verlag paul Parey.

Sutherland, R. A. (2000). Bed sediment-associated trace metals in an urban stream, Oahu. *Hawaii. Environmental Geology, 39*, 611–627. https://doi.org/10.1007/s002540050473

Soliman, F. N., Younis, M. A., Elkady, M. E., & Mohamedein, I. L. (2018). Geochemical associations, risk assessment, and source identification of selected metals in sediments from the Suez Gulf. *Egyptian Human and Ecological Risk Assessment: An International Journal, 25*(3), 738–754.

Song, J., Lui, Q., Sheng, Y. (2019a). Distribution and risk assessment of trace metals in riverine surface sediments in gold mining area. *Environmental Monitoring and Assessment, 191*, 191–203. https://doi.org/10.1007/s10661-019-7311-9

Song, J., Liu, Q., Sheng, Y. (2019b). Distribution and risk assessment of trace metals in riverine surface sediments in gold mining area. *Environmental Monitoring and Assessment, 191*(3). https://doi.org/10.1007/s10661-019-7311-9

Sun, Z., Chen, J. (2018). Risk assessment of potentially toxic elements (PTEs) pollution at a rural industrial wasteland in an abandoned metallurgy factory in north China. *International Journal Environmental Research and Public Health*, (15), 85. https://doi.org/10.3390/ijerph15010085

U.S. Environmental Protection Agency (USEPA). (2002) Supplemental guidance for developing soil screening levels for superfund sites. Washington, DC, USA: Office of Emergency and Remedial Response Document OSWER 9355–4 4 24.

U.S. Environmental Protection Agency (USEPA). (2005). Guidelines for carcinogen risk assessment.

Ustaoğlu, F., Tepe, Y., & Aydın, H. (2020). Heavy metals in sediments of two nearby streams from Southeastern Black Sea coast: Contamination and ecological risk assessment. *Environmental Forensics, 21*(2).

Ustaoğlu, F., Islam, M. D. (2020). Potential toxic elements in sediment of some rivers at Giresun, Northeast Turkey: A preliminary assessment for ecotoxicological status and health risk. *Ecological Indicators*, (113), https://doi.org/10.1016/j.ecolind.2020.106237

Üstün, E. G. (2011). The Assessment o f Heavy Metal contamination in the waters o f the Nilufer Stream in Bursa. *Ecology, 20*(81), 61–66. https://doi.org/10.5053/ekoloii.2011.819

Viard, B., Pihan, F., Promeyrat, S., & Pihan, J.-C. (2004). Integrated assessment of heavy metal (Pb, Zn, Cd) highway pollution: Bioaccumulation in soil, Graminaceae and land snails. *Chemosphere, 55*, 1349–1359.

Wang, C., Liu, S., Zhao, Q., Deng, L., & Dong, S. (2012). Spatial variation and contamination assessment of heavy metals in sediments in the Manwan Reservoir, Lancang River. *Ecotoxicology and Environmental Safety, 82*, 32–39. https://doi.org/10.1016/j.ecoenv.2012.05.006

Wang, J. Z., Peng, S. C., Chen, T. H., et al. (2016). Occurrence, source identification and ecological risk evaluation of metal elements in surface sediment: Toward a comprehensive understanding of heavy metal pollution in Chaohu Lake, Eastern China. *Environmental Science and*

Pollution Research, 23, 307–314. https://doi.org/10.1007/s11356-015-5246-4

Wei, X., Hao, M., Shao, M. (2007). Copper fertilizer effects on copper distribution and vertical transport in soils. *Geoderma*, (138). https://doi.org/10.1016/j.geoderma.2006.11.012

Wei, J., Cen, K. (2020). Assessment of human health risk based on characteristics of potential toxic elements (PTEs) contents in foods sold in Beijing, China. *Science of The Total Environment*, (703). https://doi.org/10.1016/j.scitotenv.2019.134747

Wildlife Conservation Foundation (WWF). (2014). *Turkey's water risks report*. HSBC, Istanbul Bilgi University Press.

Xiao, H., Shahab, A., Xi, B., Chang, Q., You, S., Li, J., et al. (2021). Heavy metal pollution, ecological risk, spatial distribution, and source identification in sediments of the Lijiang River, China. *Environmental Pollution*, (15), 269, 116189. https://doi.org/10.1016/j.envpol.2020.116189

Yuan, Z., Taoran, S., Yan, Z., & Tao, Y. (2014). Spatial distribution and risk assessment of heavy metals in sediments from a hypertrophic plateau lake Dianchi. *China. Environmental Monitoring and Assesment, 186*, 1219–1234.

Zhang, G., Bai, J., Zhao, Q., &, et al. (2016). Heavy metals in wetland soils along a wetland-forming chronose quence in the Yellow River Delta of China: Levels, sources and toxic risks. *Ecological Indicators., 69*, 331–339. https://doi.org/10.1016/j.ecolind.2016.04.042